Vortex Fluctuations in Underdoped $Bi_2Sr_2CaCu_2O_{8+\delta}$ Crystals

Sylvain Colson,[1] Marcin Konczykowski,[1] Marat B. Gaifullin,[2] Yuji Matsuda,[2] Piotr Gierłowski,[3] Ming Li,[4] Peter H. Kes,[4] and Cornelis J. van der Beek[1]

[1]*Laboratoire des Solides Irradiés, CNRS-UMR 7642 and CEA/DSM/DRECAM, Ecole Polytechnique, 91128 Palaiseau, France*
[2]*Institute for Solid State Physics, University of Tokyo, Kashiwanoha, Kashiwa, Chiba 277-8581, Japan*
[3]*Institute of Physics, Polish Academy of Sciences, Aleja Lotników 32/46, 02-668 Warsaw, Poland*
[4]*Kamerlingh Onnes Laboratorium, Leiden University, P.O. Box 9506, 2300 RA Leiden, the Netherlands*

(Received 15 April 2002; published 3 April 2003)

Vortex thermal fluctuations in heavily underdoped $Bi_2Sr_2CaCu_2O_{8+\delta}$ ($T_c = 69.4$ K) are studied using Josephson plasma resonance. From the zero-field data, we obtain the c-axis penetration depth $\lambda_{L,c}(0) = 230 \pm 10$ μm and the anisotropy ratio $\gamma(T)$. The low plasma frequency allows us to study phase correlations over the whole vortex solid state and to extract a wandering length r_w of vortex pancakes. The temperature dependence of r_w as well as its increase with dc magnetic field is explained by the renormalization of the vortex line tension by the fluctuations, suggesting that this softening is responsible for the dissociation of the vortices at the first order transition.

DOI: 10.1103/PhysRevLett.90.137002 PACS numbers: 74.25.Op, 74.40.+k, 74.25.Qt, 74.72.–h

Vortex thermal fluctuations are considered essential in determining the (B, T) phase diagram of layered high temperature superconductors and notably the first order transition (FOT) in which the ordered vortex crystal transforms to a liquid state without long range phase coherence [1,2]. Many scenarios, varying from vortex lattice melting described by a Lindemann criterion [3] to layer decoupling [4–6], all considering various degrees of coupling between the superconducting layers, have successfully been used to describe the position of the FOT in the (B, T) plane. However, such fits to the FOT line have not been able to convincingly discriminate between the different models. Here, we aim to do just that, through a direct measurement of the amplitude, as well as the field and temperature dependence of vortex thermal excursions in the vortex solid phase that lead to the FOT.

For this study, we use the layered $Bi_2Sr_2CaCu_2O_{8+\delta}$ (BSCCO) compound, in which vortex excursions are accessible using the Josephson plasma resonance (JPR) technique [7,8]. Briefly, the interlayer Josephson current $J_m^{(c)}$ is measured through the JPR frequency $\omega_{pl} \sim J_m^{(c)1/2}$, at which the equality of charging and kinetic energy leads to a collective excitation of Cooper pairs across the layers. In turn, $\omega_{pl}^2(B, T) = \omega_{pl}^2(0, T) \times \langle \cos(\phi_{n,n+1}) \rangle$ intimately depends on the gauge-invariant phase difference $\phi_{n,n+1}$ between adjacent layers n and $n + 1$ [9]. Here, $\langle \cdots \rangle$ stands for thermal and disorder averaging. Thus, JPR is a probe of the interlayer phase coherence. The fluctuations of vortex lines created by a dc magnetic field applied perpendicularly to the layers modify the relative phase difference between adjacent layers and thus depress ω_{pl}. In $Bi_2Sr_2CaCu_2O_{8+\delta}$, the ensemble of vortex lines should be described as stacks of two-dimensional pancake vortices. Thermal fluctuations shift the individual vortex pancakes with respect to their nearest neighbors in the c direction, by a distance $\mathbf{r}_{n,n+1} = \mathbf{u}_{n+1} - \mathbf{u}_n$. Here $\mathbf{u}_n$ is the ab-plane displacement of the pancake vortex in layer n with respect to the equilibrium position of the stack it belongs to. The wandering length of vortex lines, which is related directly to the JPR frequency ω_{pl}^2, is defined as $r_w = \langle \mathbf{r}_{n,n+1}^2 \rangle^{1/2}$ [10,11]. Below, we shall consider only temperatures above $T = 42$ K, at which vortex pinning (quenched disorder) is unimportant [2,12].

Underdoped BSCCO single crystals ($T_c = 69.4 \pm 0.6$ K) were grown by the traveling solvent floating zone method in 25 mbar O_2 partial pressure at the FOM-ALMOS center, the Netherlands [13]. The samples were postannealed for one week at 700 °C in flowing N_2. The advantage of using heavily underdoped BSCCO is that $\omega_{pl}(0, 0) \approx 61$ GHz turns out to be very low, which allows us to measure the vortex meandering over the entire (B, T) phase diagram. Samples A and B (cut from the same crystal) have dimensions $1.35 \times 1 \times 0.04$ mm^3 and $0.7 \times 0.47 \times 0.04$ mm^3, respectively. The FOT temperature T_{FOT} of these and of a third crystal (C) from the same batch, was determined by measuring the paramagnetic peak at the FOT with a miniature Hall probe magnetometer [14].

The JPR measurements were carried out using the cavity perturbation technique (on sample A) and the bolometric method (on samples A and B). For the cavity perturbation technique, the sample was glued in the center of the top cover of a cylindrical Cu cavity used in the different TM_{01i} ($i = 0, \ldots, 4$) modes. These provide the correct configuration of the microwave field at the sample location, in which $E_{\mathrm{rf}} \parallel c$ axis and $H_{\mathrm{rf}} \approx 0$ [15]. The unloaded quality factor Q_0 is measured as a function of temperature and field to obtain the power absorbed by the sample (Fig. 1). The bolometric method [16] consists of measuring the heating of the sample induced by the absorption of the incident microwave power when the JPR is excited [8,15]. The homogeneity of the dc field at the sample position was verified with a Hall probe of active

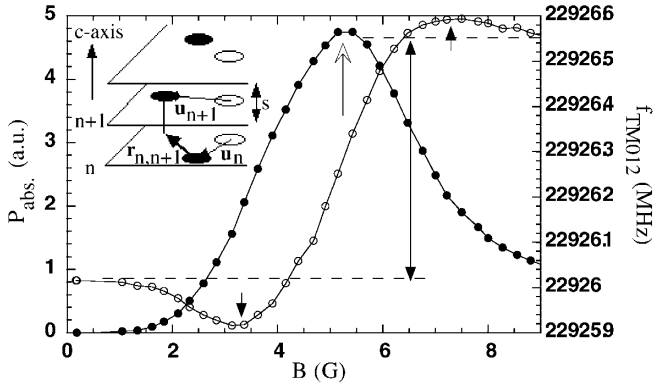

FIG. 1. Field sweep experiment on sample A at $T = 66$ K in the TM_{012} mode of the cavity ($f = 22.9$ GHz). At $B_{JPR} = 5.3$ G (open arrow), for which $\omega = \omega_{pl}$, the power absorbed in the sample (●) has a maximum and the resonance frequency of the cavity (○) shows a double-peak structure (closed arrows), and a jump (arrow between dashed lines). Inset: meandering of pancakes along a vortex line in a layered superconductor. Thermal fluctuations shift pancakes (full circles) away from their equilibrium positions (open circles).

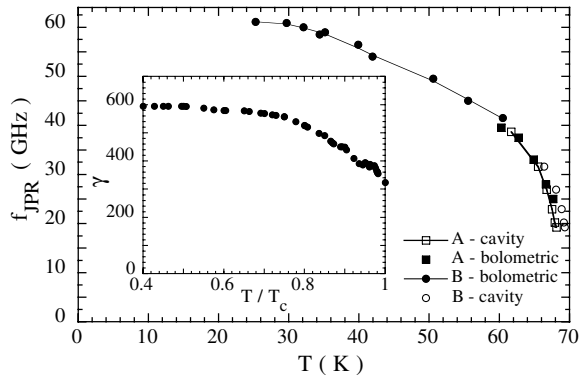

FIG. 2. JPR frequency vs temperature in $B = 0$ for samples A and B, measured by both the bolometric method and the cavity perturbation technique. We use spline fits (solid lines) in the extraction of the wandering length (see text). Inset: experimental temperature dependence of γ, obtained by the division of the experimental $\lambda_{L,c}(T)$ by the $\lambda_{L,ab}(T)$ from reversible magnetization.

area $10 \times 10\ \mu m^2$. Magneto-optical imaging of the flux distribution in the samples revealed that field inhomogeneity and irreversibility due to surface barriers can be neglected. The reversible magnetization of sample A was measured using a commercial superconducting quantum interference device magnetometer in order to extract the ab-plane London penetration depth $\lambda_{L,ab}(T)$ [13].

Figure 2 shows the JPR frequency $f_{JPR} = \omega_{pl}/2\pi$ in zero field obtained by the above-mentioned methods on samples A and B. ω_{pl}^2 is proportional to the maximum interlayer Josephson current along the c axis [9],

$$\omega_{pl}^2(B,T) = \omega_{pl}^2(0,T)\langle\cos(\phi_{n,n+1})\rangle = \frac{2\pi s}{\epsilon\Phi_0} J_m^{(c)}(B,T), \tag{1}$$

where $J_m^{(c)}(B,T) = J_m^{(c)}(0,T)\langle\cos(\phi_{n,n+1})\rangle$ is the maximum Josephson current, $s = 1.5$ nm is the interlayer spacing, ϵ the high-frequency dielectric constant, and Φ_0 the flux quantum. Using $\omega_{pl}(0,T) = 1/\lambda_{L,c}(T)\sqrt{\mu_0\epsilon}$ and $\epsilon = 11.5\epsilon_0$ [17], we obtain the London penetration depth for currents along the c axis, $\lambda_{L,c}(T)$ (ϵ_0 is the permittivity of the vacuum). When divided by the $\lambda_{L,ab}(T)$ data from reversible magnetization, this yields, without any model assumptions, the anisotropy parameter $\gamma(T) \equiv \lambda_{L,c}(T)/\lambda_{L,ab}(T)$, shown in Fig. 2. Typically, at $T = 0.5T_c$, $\lambda_{L,c} \approx 240\ \mu$m and $\lambda_{L,ab} \approx 400$ nm, so that $\gamma \approx 600$, consistent with other data for the same material [8]. Note that γ decreases as a function of temperature.

To analyze our JPR data in nonzero magnetic fields, we should divide $\omega_{pl}(B,T)$ by the zero-field result depicted in Fig. 2. In the absence of a model that satisfactorily describes $\omega_{pl}(0,T)$ over the whole temperature range, we resort to a spline fit to the experimental data. Slight differences between samples A and B were found to have a negligible influence. The vortex wandering length r_w is extracted as follows. In the single-vortex regime, at very low fields $B < B_J = \Phi_0/\lambda_J^2$, $B < B_\lambda = \Phi_0/4\pi\lambda_{L,ab}^2$, Bulaevskii and Koshelev derived [10,11]

$$1 - \frac{\omega_{pl}^2(B,T)}{\omega_{pl}^2(0,T)} \approx \frac{\pi B}{2\Phi_0} r_w^2 \ln\frac{\lambda_J}{r_w}, \tag{2}$$

where the Josephson length $\lambda_J = \gamma s$. This relation is meaningful only for small excursions $r_w \lesssim 0.6\lambda_J$, i.e., for $\langle\cos(\phi_{n,n+1})\rangle = \omega_{pl}^2(B,T)/\omega_{pl}^2(0,T) \lesssim 1$. More generally, one expects an increase of $1 - \langle\cos(\phi_{n,n+1})\rangle$ with r_w up to a plateau for large r_w, as was found in recent simulations of the evolution of $1 - \langle\cos(\phi_{n,n+1})\rangle$ versus $\langle u\rangle/a_0 \sim r_w/a_0$ for a pancake gas ($a_0 = \sqrt{\Phi_0/B}$ is the intervortex spacing) [18]. The numerical data show that $1 - \langle\cos(\phi_{n,n+1})\rangle$ is almost quadratic in r_w for $0 \lesssim 1 - \langle\cos(\phi_{n,n+1})\rangle \lesssim 0.7$–$0.8$, in agreement with Eq. (2), if the weak logarithmic dependence on λ_J/r_w is disregarded. Thus, we use

$$r_w^2 = \frac{2\Phi_0}{\pi B}(1 - \langle\cos(\phi_{n,n+1})\rangle) \tag{3}$$

to obtain an approximation of the wandering length. Since $r_w = \langle(\mathbf{u}_{n+1} - \mathbf{u}_n)^2\rangle^{1/2} = [2(u^2 - \langle\mathbf{u}_n \cdot \mathbf{u}_{n+1}\rangle)]^{1/2}$, one has, in the case of completely uncorrelated layers (e.g., for a pancake gas), $r_w = \langle 2\mathbf{u}_n^2\rangle^{1/2} \equiv \sqrt{2}u$. Disregarding the "anticorrelated" situation with $\mathbf{u}_n \cdot \mathbf{u}_{n+1} < 0$, correlations between pancake positions in different layers yield $r_w < \sqrt{2}u$, i.e., $r_w/\sqrt{2}$ is a lower limit for the root mean squared (rms) displacement u of the vortex line.

Figure 3 shows $1 - \omega_{pl}^2(B,T)/\omega_{pl}^2(0,T) = 1 - \langle\cos(\phi_{n,n+1})\rangle$ as a function of temperature in different dc fields. The temperature dependence of the wandering length r_w, obtained by applying Eq. (3), is represented in

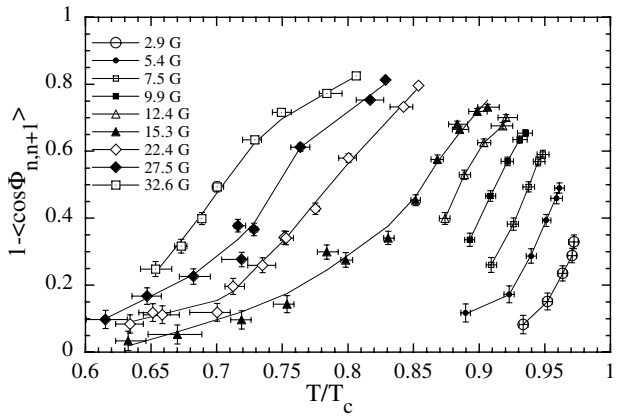

FIG. 3. $1 - \langle\cos(\phi_{n,n+1})\rangle$ vs temperature for different magnetic fields. We extract r_w from these data using Eq. (3).

Fig. 4. For every field, we observe an increase of r_w with T. At constant temperature, r_w increases with magnetic field, implying that the single-vortex part of the tilt modulus dominates the elastic energy (see below). Another interesting feature of the $r_w(T)$ curve is the break in the slope which appears at a field-dependent temperature close to the FOT and above which all the r_w curves merge into one. Alternatively, one may plot the same values of r_w vs $T/T_{\rm FOT}$ [Fig. 4(b)]. Here, two regimes appear clearly: for $T < 0.96T_{\rm FOT}$, $r_w(T/T_{\rm FOT})$ roughly overlaps for all fields, whereas for $T > 0.96T_{\rm FOT}$, the curves deviate from each other. This shows that in the vortex solid, r_w depends on temperature as $r_w(T/T_{\rm FOT})$.

We now discuss the temperature and field dependence of r_w in the vortex solid. The rms thermal vortex displacement u can be obtained by equipartition of the associated elastic energy with the thermal energy, $U_{el} = c_{44}a_0^2(u^2/s) = k_BT$. The vortex lattice tilt modulus

$$c_{44}(\mathbf{k}) \approx \frac{B^2/\mu_0}{1 + \lambda_c^2 k_\parallel^2 + \lambda_{ab}^2 Q_z^2} + \frac{\varepsilon_0}{2\gamma^2 a_0^2}\ln\frac{k_{\rm max}^2}{K_0^2 + (Q_z/\gamma)^2} + \frac{\varepsilon_0}{2\lambda_{ab}^2 Q_z^2 a_0^2}\ln\left(1 + \frac{a_0^2}{21.3 r_w^2}\right), \quad (4)$$

calculated by Koshelev and Vinokur [19] and Goldin and Horovitz [20], consists of three terms: the nonlocal collective (lattice) term, the vortex line tension term, determined by Josephson coupling between layers, and a third term due to the electromagnetic dipole interaction between pancakes. Of particular interest here is the logarithmic correction to the temperature dependence of the second term, introduced by the cutoff $k_{\rm max} = \pi/r_w$, which corresponds to the smallest meaningful deformation [19,20]. To proceed, we evaluate U_{el} at the typical vortex line deformation wave vectors parallel and perpendicular to the layers, $k_\parallel \approx \pi/u$ and $Q_z \approx \pi\gamma/2a_0 \ll 2\pi/s$. Writing $K_0 = \sqrt{4\pi}/a_0$, $r_w^2 = \alpha u^2$ (with $\alpha \approx 1$) and $x = a_0/r_w$, equipartition yields

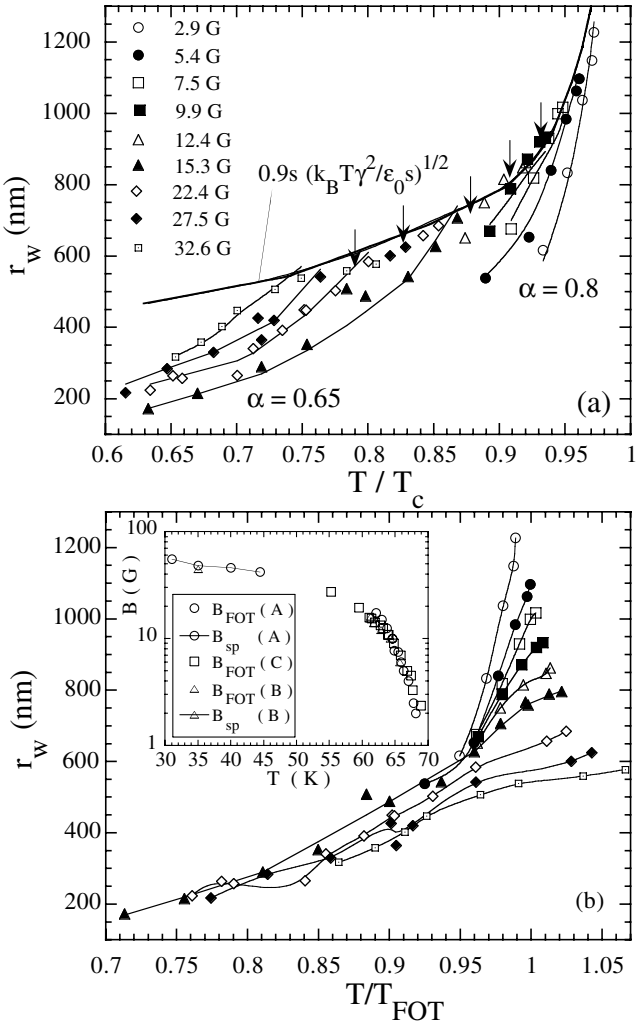

FIG. 4. (a) Experimental r_w vs T/T_c for different magnetic fields in strongly underdoped BSCCO. For $B = 27.5$, 22.4, 15.3, 12.4, and 9.9 G, arrows show the temperature of the FOT. The thick line shows the evolution of $0.9s(k_BT\gamma^2/\varepsilon_0 s)^{1/2}$. Thin lines are fits to Eq. (5) with $\alpha = 0.8$ (for $B < 15$ G) and $\alpha = 0.65$, omitting the term $4/\pi(\alpha x^2 + \frac{1}{4})$ ($B > 15$ G). (b) r_w vs $T/T_{\rm FOT}$. Solid lines are guides to the eye. Inset: phase diagram of the samples used in this study, showing the position of the FOT line as revealed by the paramagnetic peak in the local susceptibility ($B_{\rm FOT}$) or the second peak in the dc magnetization (B_{sp}).

$$r_w^2 \approx \alpha s^2 \frac{k_BT\gamma^2}{\varepsilon_0 s}\left[\frac{4}{\pi(\alpha x^2 + \frac{1}{4})} + \frac{1}{2}\ln(0.66x^2) + \frac{2}{\pi^2}\left(\frac{a_0}{\lambda_{L,ab}}\right)^2\ln\left(1 + \frac{x^2}{21.3}\right)\right]^{-1}. \quad (5)$$

All parameters in Eq. (5), and notably $\varepsilon_0(T)/\gamma^2(T) = \Phi_0^2/4\pi\mu_0\lambda_{L,c}^2$, are known from experiment, which allows a direct comparison to the $r_w(T)$ data. For the lowest four fields ($B < 10$ G), the line tension term is largest all the way to the FOT. Equation (5), which then reduces to Eq. (40) of Ref. [20] with $Q_z \approx \pi\gamma/2a_0$ instead of

$2\pi/s$, very well describes the magnitude, the temperature, as well as the field dependence of r_w, using the single free parameter $\alpha = 0.8$. For higher fields, the nonlocal collective contribution to c_{44} increases, eventually exceeding the Josephson coupling (line tension) term close to the FOT for $B > 20$ G. However, the inclusion of the nonlocal term leads to too weak a temperature dependence of $r_w(T)$. Rather, the experimental wandering length behaves as if the line tension term dominates the vortex response at all fields [11]: excellent fits of both the temperature and field dependence are obtained by omitting the nonlocal collective term [i.e., $4/\pi(\alpha x^2 + \frac{1}{4})$ in Eq. (5)] and using $\alpha = 0.65$; see Fig. 4(a). Note that while the main $r_w(T)$ dependence comes from the prefactor $\gamma^2 T/\varepsilon_0$ in Eq. (5) [thick line in Fig. 4(a)], the behavior of r_w in the vortex solid can be understood as the result of the logarithmic correction arising from the softening of the line tension term by thermal fluctuations [19,20]. The field dependence comes from the zone-boundary vector K_0 and the small Q_z, indicating that vortex lines are correlated (linelike) on distances that well exceed the layer spacing s.

An increase of r_w with increasing vortex density can arise from the suppression of Josephson coupling by vortex fluctuations or from the weaker interpancake dipole coupling, but is incompatible with a dominant role of the shear energy or of compressional or collective tilt modes and thus with Lindemann-like melting [3]. Moreover, using our experimental data to compare the different contributions to the elastic energy, we find that the dipole coupling and the shear energy are, under all circumstances, negligible. Thus, dislocation-mediated (Kosterlitz-Thouless–like) melting, as well as vortex line evaporation [6] are also unlikely. Rather, the large thermal excursions of pancake vortices soften the line tension contribution to c_{44} for the large-wave vector modes that lead to the FOT. This complies with recent measurements showing that vortex lattice order is not a prerequisite for the FOT [21]. For deformations with smaller wave vectors, Josephson coupling still contributes to the line tension even in the vortex liquid, leading to, e.g., the anisotropic vortex response to columnar defects in heavy-ion irradiated samples. These conclusions, arrived at for extremely anisotropic underdoped BSCCO, will also hold for less anisotropic *layered* superconductors.

Summarizing, JPR measurements on heavily underdoped BSCCO crystals yield the c-axis penetration depth, the anisotropy parameter $\gamma(T)$, and the wandering length r_w of vortex lines. The observed temperature and field dependences of r_w suggest that thermal fluctuations soften the Josephson coupling contribution to the tilt modulus for short wavelengths [20], a softening that we believe drives the FOT.

We thank the European Science Foundation VORTEX program and the Nederlandse Organisatie voor Wetenschappelijk Onderzoek for financial support. P. G. acknowledges support of the Polish Government, Grant No. PBZ-KBN-013/T08/19.

[1] R. Cubitt, E. M. Forgan, G. Yang, S. L. Lee, D. McK. Paul, H. A. Mook, M. Yethiraj, P. H. Kes, T. W. Li, A. A. Menovsky, Z. Tarnawski, and K. Mortensen, Nature (London) **365**, 407 (1993).

[2] E. Zeldov, D. Majer, M. Konczykowski, V. B. Geshkenbein, V. M. Vinokur, and H. Shtrikman, Nature (London) **375**, 373 (1995).

[3] G. Blatter, V. B. Geshkenbein, A. I. Larkin, and H. Nordborg, Phys. Rev. B **54**, 72 (1996).

[4] L. Glazman and A. E. Koshelev, Phys. Rev. B **43**, 2835 (1991).

[5] L. L. Daemen, L. N. Bulaevskii, M. P. Maley, and J. Y. Coulter, Phys. Rev. Lett. **70**, 1167 (1993).

[6] M. J. W. Dodgson, A. E. Koshelev, V. B. Geshkenbein, and G. Blatter, Phys. Rev. Lett. **84**, 2698 (2000).

[7] Y. Matsuda, M. B. Gaifullin, and K. Kumagai, Phys. Rev. Lett. **75**, 4512 (1995); Y. Matsuda, M. B. Gaifullin, K. Kumagai, M. Kosugi, and K. Hirata, Phys. Rev. Lett. **78**, 1972 (1997); T. Shibauchi, T. Nakano, M. Sato, T. Kisu, N. Kameda, N. Okuda, S. Ooi, and T. Tamegai, Phys. Rev. Lett. **83**, 1010 (1999).

[8] M. B. Gaifullin, Yuji Matsuda, N. Chikumoto, J. Shimoyama, and K. Kishio, Phys. Rev. Lett. **84**, 2945 (2000).

[9] L. N. Bulaevskii, M. P. Maley, and M. Tachiki, Phys. Rev. Lett. **74**, 801 (1995).

[10] L. N. Bulaevskii, A. E. Koshelev, V. M. Vinokur, and M. P. Maley, Phys. Rev. B **61**, R3819 (2000).

[11] A. E. Koshelev and L. N. Bulaevskii, Physica (Amsterdam) **341C–348C**, 1503 (2000).

[12] N. Avraham, B. Khaykovich, Y. Myasoedov, M. Rappaport, H. Shtrikman, D. E. Feldman, T. Tamegai, P. H. Kes, Ming Li, M. Konczykowski, C. J. van der Beek, and E. Zeldov, Nature (London) **411**, 451 (2001).

[13] Ming Li, C. J. van der Beek, M. Konczykowski, A. A. Menovsky, and P. H. Kes, Phys. Rev. B **66**, 024502 (2002).

[14] N. Morozov, E. Zeldov, D. Majer, and M. Konczykowski, Phys. Rev. B **54**, R3784 (1996).

[15] S. Colson, C. J. van der Beek, M. Konczykowski, M. B. Gaifullin, Y. Matsuda, P. Gierlowski, Ming Li, and P. H. Kes, Physica (Amsterdam) **369C**, 236 (2002).

[16] Y. Matsuda, N. P. Ong, Y. F. Yan, J. M. Harris, and J. B. Peterson, Phys. Rev. B **49**, 4380 (1994).

[17] M. B. Gaifullin, Y. Matsuda, N. Chikumoto, J. Shimoyama, K. Kishio, and R. Yoshizaki, Physica (Amsterdam) **362C**, 228 (2001).

[18] E. H. Brandt and E. B. Sonin, Phys. Rev. B **66**, 064505 (2002).

[19] A. E. Koshelev and V. M. Vinokur, Phys. Rev. B **57**, 8026 (1998).

[20] T. R. Goldin and B. Horovitz, Phys. Rev. B **58**, 9524 (1998).

[21] S. S. Banerjee, A. Soibel, Y. Myasoedov, M. Rappaport, E. Zeldov, M. Menghini, Y. Fasano, F. de la Cruz, C. J. van der Beek, and M. Konczykowski, Phys. Rev. Lett. **90**, 087004 (2002).